Taylor & Francis
Taylor & Francis Group

Journal of Toxicology and Environmental Health, Part A
Current Issues

ISSN: 1528-7394 (Print) 1087-2620 (Online) Journal homepage: http://www.tandfonline.com/loi/uteh20

Pulmonary toxicity and global gene expression changes in response to sub-chronic inhalation exposure to crystalline silica in rats

Christina Umbright, Rajendran Sellamuthu, Jenny R. Roberts, Shih-Houng Young, Diana Richardson, Diane Schwegler-Berry, Walter McKinney, Bean Chen, Ja Kook Gu, Michael Kashon & Pius Joseph

To cite this article: Christina Umbright, Rajendran Sellamuthu, Jenny R. Roberts, Shih-Houng Young, Diana Richardson, Diane Schwegler-Berry, Walter McKinney, Bean Chen, Ja Kook Gu, Michael Kashon & Pius Joseph (2017) Pulmonary toxicity and global gene expression changes in response to sub-chronic inhalation exposure to crystalline silica in rats, Journal of Toxicology and Environmental Health, Part A, 80:23-24, 1349-1368, DOI: 10.1080/15287394.2017.1384773

To link to this article: https://doi.org/10.1080/15287394.2017.1384773

JOURNAL OF TOXICOLOGY AND ENVIRONMENTAL HEALTH, PART A
2017, VOL. 80, NOS. 23–24, 1349–1368
https://doi.org/10.1080/15287394.2017.1384773

Taylor & Francis
Taylor & Francis Group

Pulmonary toxicity and global gene expression changes in response to sub-chronic inhalation exposure to crystalline silica in rats

Christina Umbright, Rajendran Sellamuthu, Jenny R. Roberts, Shih-Houng Young, Diana Richardson, Diane Schwegler-Berry, Walter McKinney, Bean Chen, Ja Kook Gu, Michael Kashon, and Pius Joseph

Toxicology and Molecular Biology Branch, Health Effects Laboratory Division, National Institute for Occupational Safety and Health (NIOSH), Morgantown, WV, USA

ABSTRACT

Exposure to crystalline silica results in serious adverse health effects, most notably, silicosis. An understanding of the mechanism(s) underlying silica-induced pulmonary toxicity is critical for the intervention and/or prevention of its adverse health effects. Rats were exposed by inhalation to crystalline silica at a concentration of 15 mg/m^3, 6 hr/day, 5 days/week for 3, 6 or 12 weeks. Pulmonary toxicity and global gene expression profiles were determined in lungs at the end of each exposure period. Crystalline silica was visible in lungs of rats especially in the 12-week group. Pulmonary toxicity, as evidenced by an increase in lactate dehydrogenase (LDH) activity and albumin content and accumulation of macrophages and neutrophils in the bronchoalveolar lavage (BAL), was seen in animals depending upon silica exposure duration. The most severe histological changes, noted in the 12-week exposure group, consisted of chronic active inflammation, type II pneumocyte hyperplasia, and fibrosis. Microarray analysis of lung gene expression profiles detected significant differential expression of 38, 77, and 99 genes in rats exposed to silica for 3-, 6-, or 12-weeks, respectively, compared to time-matched controls. Among the significantly differentially expressed genes (SDEG), 32 genes were common in all exposure groups. Bioinformatics analysis of the SDEG identified enrichment of functions, networks and canonical pathways related to inflammation, cancer, oxidative stress, fibrosis, and tissue remodeling in response to silica exposure. Collectively, these results provided insights into the molecular mechanisms underlying pulmonary toxicity following sub-chronic inhalation exposure to crystalline silica in rats.

ARTICLE HISTORY
Received 18 July 2017
Accepted 22 September 2017

KEYWORDS
Crystalline silica; inhalation exposure; pulmonary toxicity; gene expression; mechanisms

Introduction

Silica is one of the most abundant minerals present in the earth's crust. Among the various forms of silica, crystalline silica is the most important, from a toxicological perspective. Crystalline silica interacts with the biological systems to result in toxicity. Crystalline silica exposure was found to result in toxicity in *in vitro* cell culture systems (Sellamuthu et al. 2011a) and *in vivo* animal models (Sellamuthu et al. 2012, 2011b; Shi et al. 1998). In addition, a definite relationship was established between exposure to crystalline silica and adverse health effects among workers (Cooper, Miller, and Germolec 2002; Madl et al. 2008; Steenland and Goldsmith 1995).

Occupational exposure to crystalline silica and resulting adverse health effects are the major concerns for the World Health Organization (WHO), International Labor Organization (ILO), Occupational Safety and Health Administration (OSHA), and National Institute for Occupational Safety and Health (NIOSH). Any occupation that involves the movement of earth results in generation of dust containing crystalline silica. Depending upon the type of activity and composition of dust, the amount of crystalline silica present in dust varies. Occupations such as farm work generate only limited amounts of crystalline silica containing dust. On the other hand, occupations such as construction, mining, sand blasting, drilling, and hydraulic fracturing (fracking) generate large quantities of dust potentially resulting in exposure to substantial concentrations of

CONTACT Pius Joseph pcj5@cdc.gov MS 3014, Toxicology and Molecular Biology Branch, National Institute for Occupational Safety and Health (NIOSH), 1095 Willowdale Road, Morgantown, WV 26505, USA.

Color versions of one or more of the figures in the article can be found online at www.tandfonline.com/uteh
Supplemental data for this article can be accessed at the publisher's website.

crystalline silica among workers who are employed in such occupations (Madl et al. 2008).

Crystalline silica is toxic and, therefore, occupational exposure to dust containing crystalline silica is a major health threat for millions of workers. An association between excessive exposure to crystalline silica and diseases such as cancer (Gulumian et al. 2006; IARC 1997; Shi et al. 1998), autoimmune diseases (Steenland and Goldsmith 1995), tuberculosis (Rees and Murray 2007), and renal disease (Vupputuri et al. 2012) was reported. Silicosis, a potentially fatal and irreversible, but preventable chronic obstructive pulmonary disease, is the most consequential adverse health effect associated with occupational exposure to crystalline silica (Hnizdo and Vallyathan 2003). The single most effective strategy to prevent silicosis is to avoid exposure to dust containing silica. The NIOSH Recommended Exposure Limit (REL) for crystalline silica is 50 μg/m^3 (NIOSH 2002). In order to adequately protect workers from developing adverse health effects associated with their occupational exposure to silica, OSHA (2016) proposed to lower the Permissible Exposure Limit (PEL) of respirable crystalline silica to an 8-hr-time-weighted average in all industries from 100 μg/m^3 to 50 μg/m^3. Workers in certain occupations; however, are exposed to crystalline silica at higher levels, reaching 100-fold higher compared to the current PEL of 100 μg/m^3 (Esswein et al. 2013). Exposures to excessive quantities of crystalline silica may account for the death of over 100 workers/year in the US (Mazurek et al. 2015) and thousands of new cases being reported worldwide (Leung, Yu, and Chen 2012).

Besides avoiding exposure to dust containing excess crystalline silica, detection of silica exposure, even prior to the appearance of the earliest clinically detectable symptoms of the disease, is critical for its prevention. By employing a rat inhalation exposure/toxicity model, Sellamuthu et al. (2011b) previously demonstrated that application of blood gene expression profiling was a highly sensitive surrogate approach to detect early pulmonary toxicity associated with crystalline silica exposure. A blood gene expression signature consisting of seven genes was able to distinguish silica exposed from air-exposed control rats. In addition to early detection, a comprehensive understanding of the mechanism(s) underlying development of silicosis has important implications in prevention as well as management of this disease. Global gene expression profiling by employing microarray, or newer sequencing platforms, and bioinformatic analysis of gene expression data were noted to show great promise in determining the molecular mechanisms underlying the toxicity associated with exposure to toxic agents (Guo et al. 2012; Huang 2013; Klaper et al. 2014; Sellamuthu et al. 2012, 2013). Currently, by employing a rat inhalation exposure model for silica-induced sub-chronic pulmonary toxicity, the aim of this study was to investigate the molecular mechanisms underlying lung damage.

Materials and methods

Silica aerosol generation and rat inhalation exposure system

Min-U-Sil 5 silica obtained from US Silica (Berkley Springs, WV) was used to generate an aerosol for rat inhalation exposures. The silica aerosol generation and whole body rat inhalation exposure system were designed and fabricated in the Health Effects Laboratory Division, NIOSH (Morgantown, WV) and details were described previously (McKinney, Chen, and Frazer 2009). A Venturi dispenser installed downstream of the aerosol generator facilitated dispersion of silica agglomerates to respirable particles of smaller, respirable size (Figure 1A). The mass median diameter of the silica particles employed in inhalation exposure was 1.6 μm with a geometric standard deviation of 1.6 (Figure 1B) which is within the respirable range recommended for rats. The alveolar deposition of silica was estimated as described previously (Chen et al. 2012), utilizing concentration of particles in the chamber, exposure period, minute volume for rats, and size distribution of silica particles. The aerosol generation and rat inhalation exposure system was fully automated with a computer controlling aerosol generation and delivery of uniformly dispersed airborne silica particles in addition to temperature and humidity within the exposure chamber.

Exposure of rats to crystalline silica aerosol

Approximately 3-months old, pathogen-free, male Fischer 344 rats (CDF strain) weighing

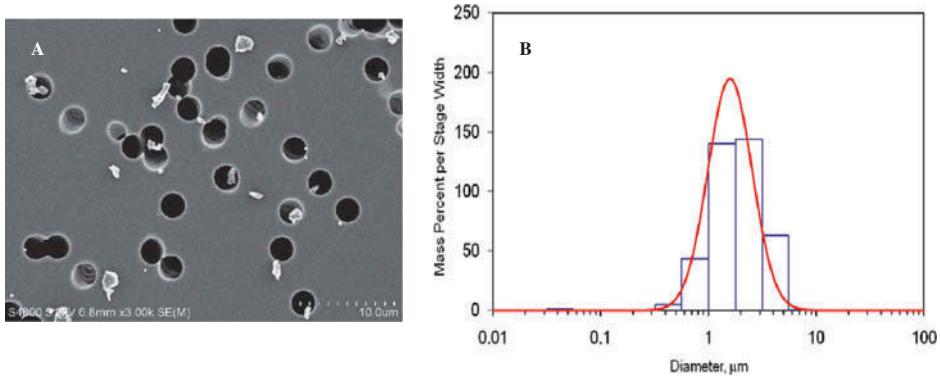

Figure 1. Characteristics of aerosol containing crystalline silica particles generated for inhalation exposure of rats. A. Scanning electron micrograph showing the sizes of crystalline silica particles generated with the Venturi de-agglomerator/dilutor in the inhalation exposure system, and B. Mass size distribution of particles determined with a MOUDI impactor.

approximately 200 g were purchased from Charles River Laboratories (Wilmington, MA) and used to conduct the studies in our AAALAC International accredited facility (NIOSH, Morgantown, WV) following an Institutional Animal Care and Use Committee approved protocol. The rats, upon arrival, were allowed to acclimate for approximately 10 days prior to utilization. Subsequently, groups of rats (n = 8) were exposed to filtered air or an aerosol containing crystalline silica at a concentration of 15 mg/m^3, 6 hr/day, 5 days/week for 3, 6 or 12 weeks. During the entire exposure period, the target levels of temperature (22.2–25.6°C), humidity (40–60%), and silica concentration (15 ± 1 mg/m^3) were monitored and maintained. Throughout the experiment, animals were maintained on a 12-hr light-dark cycle with food and tap water provided *ad libitum* except during the 6-hr silica treatment.

Pulmonary toxicity parameter determination

Approximately 16 hr following conclusion of 3, 6, or 12 weeks exposure to air or silica, rats were injected intraperitoneally (ip)with a lethal dose of sodium pentobarbital (>100 mg/kg body weight), (Fort Dodge Animal Health, Fort Dodge, IA). Blood drawn directly from the abdominal aorta was transferred to Vacutainer tubes (Becton-Dickinson, Franklin Lakes, NJ) containing EDTA as an anticoagulant and further processed to determine hematological parameters as described below. After exsanguination, right lungs were clamped off and bronchoalveolar lavage (BAL) was performed on the left lung as previously described (Antonini and Roberts 2007). Cellular and acellular fractions of BAL fluid (BALF) collected from the left lung were used for further biochemical analysis of lung injury and inflammation. The diaphragmatic and cardiac lobes of right lung were inflated and preserved in 10% neutral-buffered formalin for histopathological analysis of injury, while the apical lobe was cut into pieces and stored in RNAlater (Invitrogen, Carlsbad, CA) for utilization in gene expression studies as described below.

Biochemical analysis of pulmonary toxicity and inflammation

Lactate dehydrogenase (LDH) activity, a general indicator of pulmonary toxicity, and albumin content, an indicator of alveolar epithelial integrity, were determined in the acellular fraction of BALF using a COBAS MIRA autoanalyzer (Roche Diagnostic Systems, Mont Clair, NJ) as described previously (Antonini and Roberts 2007; Porter et al. 2001). The cellular fraction of BALF was re-suspended in 1 ml phosphate buffered saline and total number of cells and alveolar macrophages (AM) determined using a Coulter Multisizer II and Accu Comp software (Coulter Electronics, Hialeah, FL). BALF cells were deposited onto a microscope slide using a Cytospin 3 centrifuge (Shandon Life Sciences International, Cheshire, UK) and stained with a Leukostat stain (Fisher Scientific, Pittsburgh, PA) to differentiate cells. Two hundred cells were counted per rat, and

alveolar macrophage (AM) and polymorphonuclear leukocyte (PMN) % multiplied back across the total cell count to obtain total AM and PMN counts and differential PMN counts.

Hematology

By employing a flow cytometer method using antibodies specific to rat blood cells (BD Pharmingen, San Diego, CA), total and differential white blood cell (WBC) counts of un-clotted blood samples were determined. By forward and side scattering, leukocytes were separated into three gates (lymphocytes, monocytes, and neutrophils). Data were analyzed using a FlowJo software (Treestar, Costa mesa, CA) after collecting 3500 counting beads.

Lung histology

The diaphragmatic and cardiac lobes of lungs preserved in 10% neutral buffered formalin were subsequently embedded in paraffin, sectioned at a thickness of 5 μm and stained with hematoxylin and eosin (H&E) or Mason's trichrome stain. The slides were assessed for histological changes (H&E stain) or fibrosis (trichrome stain) by a board-certified pathologist (Experimental Pathology Laboratory, Inc., Sterling, VA). The lung sections were scored on a 1–4 scale where 1 = minimal, 2 = mild, 3 = moderate, and 4 = severe. Lung sections were also examined using a polarized light microscope for the presence of birefringent crystalline silica particles.

RNA isolation and determination of global gene expression profile

Total RNA was isolated from a piece of the apical lung lobe using RNeasy Fibrous Mini Kit (Qiagen Inc., Valencia, CA) as described previously (Sellamuthu et al. 2012). The fibrous kit facilitated better homogenization and yield of RNA from the lung tissue samples. The RNA samples were digested with RNase-free DNase and further purified utilizing the RNeasy Kit (Qiagen Inc., Valencia, CA). The integrity and purity of RNA samples isolated from lungs were determined employing an Agilent 2100 Bioanalyzer (Agilent Technologies, Palo Alto, CA) and RNA was quantitated by UV-Vis spectrophotometry. Only RNA samples exhibiting an RNA Integrity Number (RIN) >8.0 were used to determine global gene expression profiles.

RatRef-12 V1.0 Expression BeadChip microarray (Illumina, Inc, San Diego, CA), as described by Sellamuthu et al. (2011b), was employed to determine global gene expression profiles of RNA samples purified from lung samples. All microarray experiments were performed to comply with Minimal Information About a Microarray Experiment (MIAME) protocols (Brazma et al. 2001). Biotin-labeled cRNA was generated from 375 ng RNA per sample by employing the Illumina TotalPrep RNA Amplification Kit (Ambion, Inc, Austin, TX). Chip hybridizations, washing, Cy3-streptavidin staining, and scanning of chips on the BeadStation 500 platform (Illumina, Inc, San Diego, CA) were performed following the protocols provided by Illumina, Inc. Prior to loading samples into Beadstudio (Framework version 3.0.19.0) Gene Expression module v.3.0.14, the metrics files from the bead scanner were checked to ensure that all samples fluoresced at comparable levels. Housekeeping, hybridization control, stringency and negative control genes were checked for proper chip detection. BeadArray expression data were then exported with mean fluorescent intensity across like beads and bead variance estimates into flat files for subsequent analysis.

Illumina BeadArray expression data was analyzed in Bioconductor using the 'lumi' and 'limma' packages. Bioconductor is a project for analysis and comprehension of genomic data and operates in R, a statistical computing environment (Ihaka and Gentleman 1996). The 'lumi' Bioconductor package was specifically developed to process Illumina microarrays and encompasses data input, quality control, variance stabilization, normalization, and gene annotation (Gentleman et al. 2004). Normalized data were then analyzed using the 'limma' package in R. Briefly, limma fits a linear model for each gene, generates group means of expression, and calculates p-values and log fold-changes which are converted to standard fold changes. The raw p values were corrected for false discovery rate (FDR) using the Benjamini and Hochberg (1995) procedure. The differentially

expressed genes identified using a rather stringent selection filter (fold change in expression >1.5 and FDR p value <0.05) were considered as significantly differentially expressed genes (SDEG) and used in the bioinformatic analysis.

Quantitative real-time PCR confirmation of microarray data

Sixteen of the SDEG identified by microarray analysis in the silica exposed lung samples, compared with corresponding controls, were randomly selected for quantitative real-time PCR (QRT-PCR) analysis to confirm differential expressions. The nucleotide sequences of primers used in the QRT-PCR analysis of the target genes and house-keeping gene (β-actin) are presented in Supplementary Table 1. The QRT-PCR amplification, detection of the amplified PCR products, and their quantitation were conducted utilizing a 7900 HT Fast Real Time PCR machine and SYBR Green PCR MasterMix (Applied Biosystems, Foster City, CA). The specificity and integrity of the PCR products were determined by analyzing the dissociation curves of PCR amplified gene products. Expression levels of target genes were normalized using β-actin, the house-keeping gene, and fold changes in expression in the silica exposed samples compared with air exposed controls were calculated using the formula 2^(-(ΔCt_target gene - ΔCt_housekeeping gene).

Bioinformatic analysis of gene expression data

The SDEG identified were used as input for subsequent bioinformatics analysis using Ingenuity Pathway Analysis (IPA, Ingenuity Systems, www.ingenuity.com). IPA software is designed to map the biological relationship of uploaded genes and classify them into categories according to published literature in the database. Fisher's exact test was conducted to calculate p-value to determine the significance of a particular biological function or canonical pathway enriched by silica exposure in the lungs ($p < 0.05$ was considered statistically significant).

Statistical analysis of the data

Non-microarray data between silica exposed and controls were compared using one-way ANOVA test. Post hoc comparisons were conducted using Fisher's least significant difference (LSD) test. The level of statistical significance was set at $p < 0.05$.

Results

Calculated pulmonary deposition of crystalline silica in rats: Cumulative crystalline silica exposure estimated for rats belonging to the 3-, 6-, and 12-weeks groups was 1363 (mg/m^3) x hr, 2676 (mg/m^3) x hr, and 5389 (mg/m^3) x hr, respectively (Table 1). Inhalation treatment with crystalline silica, under the exposure conditions employed in this study, resulted in lung deposition of inhaled silica particles. This was evident from detection of birefringent crystalline silica, observed only in BALF cells and lungs of the silica exposed animals, especially those treated for the longest exposure duration of 12 weeks (Figure 2). Under polarized light microscopy, these particles were not detected in rats from the 3-week exposure group; and the amount of crystalline silica found in lung sections after 12-weeks was markedly higher compared to 6-weeks. The estimated amounts of crystalline silica deposited in the pulmonary alveolar region following 3-, 6-, or 12-weeks were 1.45 mg, 2.85 mg, and 5.74 mg, respectively (Table 1).

Table 1. Inhalation exposure and estimated alveolar deposition of crystalline silica in rats.

Group	Mean Concentration (mg/m^3)	Mean exposure/day (minutes)	Total exposure (mg/m^3)xhour	Total alveolar deposition (mg)*	Human equivalence (years)**
3 Weeks	14.9	366	1363	1.45	13.4 (26.8)
6 Weeks	14.5	369	2676	2.85	26.3 (52.6)
12 Weeks	14.9	361	5389	5.74	53 (106)

*The following assumptions were used in calculating the total alveolar deposition: crystalline silica particle deposition efficiency for rat = 8.3% and human = 11%; minute volume for rat = 0.21L and human = 20L; and alveolar epithelium surface area for rat = 0.40 m^2 and human = 102.2 m^2

**The human equivalence is calculated using the current PEL (100 μg/m^3) for crystalline silica. The numbers in the parenthesis represent those calculated using the proposed PEL (50 μg/m^3) for crystalline silica.

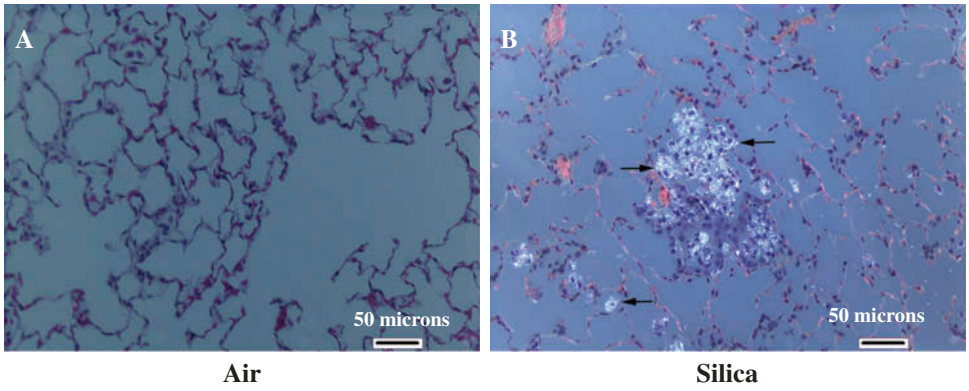

Figure 2. Photomicrographs illustrating deposition of crystalline silica particles in rat lungs. Lung sections of rats exposed by inhalation to either air (A) or crystalline silica particles (B) were prepared and stained with H&E as described in the materials and methods section. The arrows show the presence of birefringent material representing crystalline silica detected by polarizing light microscope in the lungs of the silica exposed rats. Magnification - 200X.

These correspond to 26.8, 52.6, and 106 years of human exposure calculated using the 8-hr time weighted average (TWA) of 50 μg/m^3 for crystalline silica recommended by OSHA (2016).

Pulmonary toxicity in silica exposed rats: LDH activity and albumin content in BALF following silica treatment was significantly higher compared with time-matched controls (Figure 3 A and 3B) suggesting induction of pulmonary toxicity. Significant increases in numbers of BALF cells including AM and PMN were observed in silica exposed lung samples compared to corresponding controls (Figure 3C and **3D**). In addition, BALF inflammatory cell accumulation correlated with

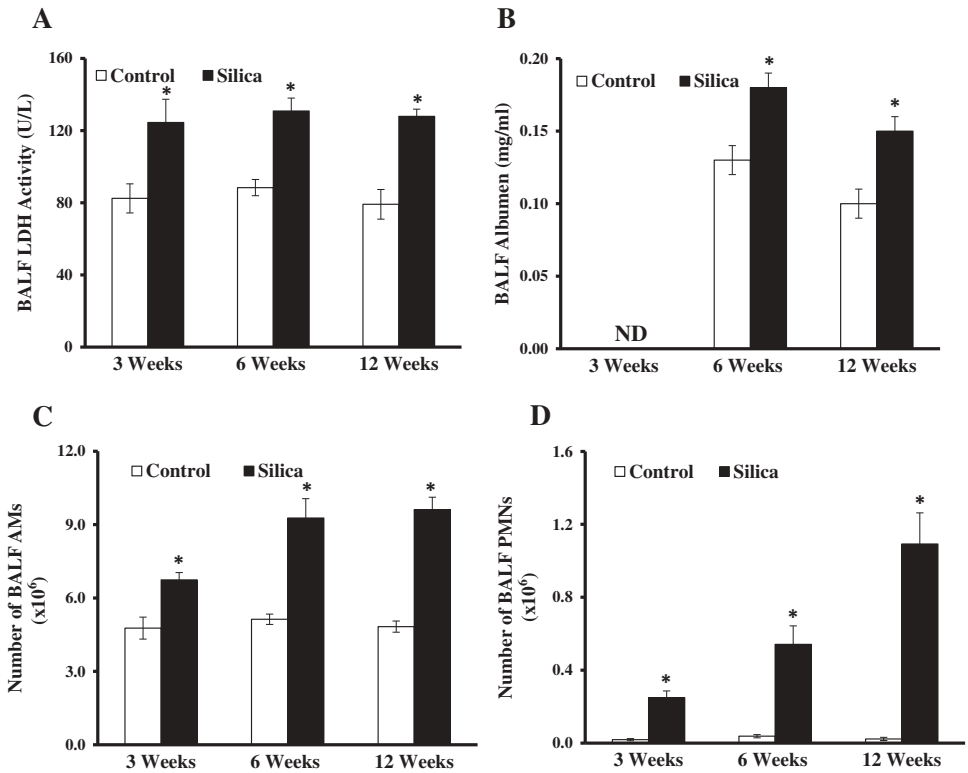

Figure 3. BAL parameters of pulmonary toxicity in the rats. Rats were exposed to air or crystalline silica particles by inhalation and the various BAL parameters of pulmonary toxicity, viz. LDH activity (A), albumin content (B), number of AM (C) and number of infiltrating PMNs (D), were determined as described under materials and methods section. Values represent mean ± S.E. (n = 8). *significantly different from time-matched controls ($p < 0.05$). ND – Not determined.

the amount of silica deposited in lungs. Histological analysis of lung sections further supported silica-induced pulmonary toxicity in exposed animals. None of the control groups of rats exhibited apparent observable pulmonary pathology and lesions. Similarly, no histopathologic changes were detected in any of rats in the 3-week silica exposure group (data not presented). Among the 8 silica exposed rats in the 6-week group, 2 exhibited minimal inflammation consisting of a few macrophages and neutrophils within the alveolar space and septa (data not presented). Minimal to mild pathologic changes were noted in all eight rats after 12-week silica treatment (Figure 4A and 4B). The inflammation found in the lungs of these rats was characterized as chronic-active and consisted of aggregates of foamy macrophages, a few lymphocytes, and rare degenerative neutrophils admixed with necrotic epithelial cells. Occasionally in areas of inflammation the alveolar septa were lined by plump, cuboidal epithelial cells (type-II pneumocyte hyperplasia). The macrophages displayed abundant, foamy to grainy cytoplasm which when exposed to polarized light contained low amounts of the birefringent material, crystalline silica (Figure 2). In addition, the septa were expanded by minimal quantities of fibrosis that was only evident upon examination with Mason's trichrome stain (Figure 4C and 4D). In spite of the evidence for silica- induced pulmonary toxicity, during the entire course of the study, animals belonging to each of the silica exposure groups (3-, 6-, and 12-weeks) exhibited physical activity, food and water consumption, and body weight gains comparable to corresponding time-matched, air-only exposed controls.

Hematological changes in silica exposed rats: Compared with time-matched controls, the total number of neutrophils detected in blood was significantly higher in all three silica treated groups (Figure 5A). The number of natural killer (NK) cells present in blood of silica exposed, compared with corresponding controls, was numerically lower in all the three treatment groups which reached significance only at 12-weeks (Figure 5B). No other hematological parameters determined exhibited any significant change related to silica exposure (data not shown). The decline in the number of NK cells detected in the blood samples of silica exposed rats, especially those belonging to the 12-week exposure group, is in agreement with a previous study that reported a reduction in the number of NK cells in silicosis

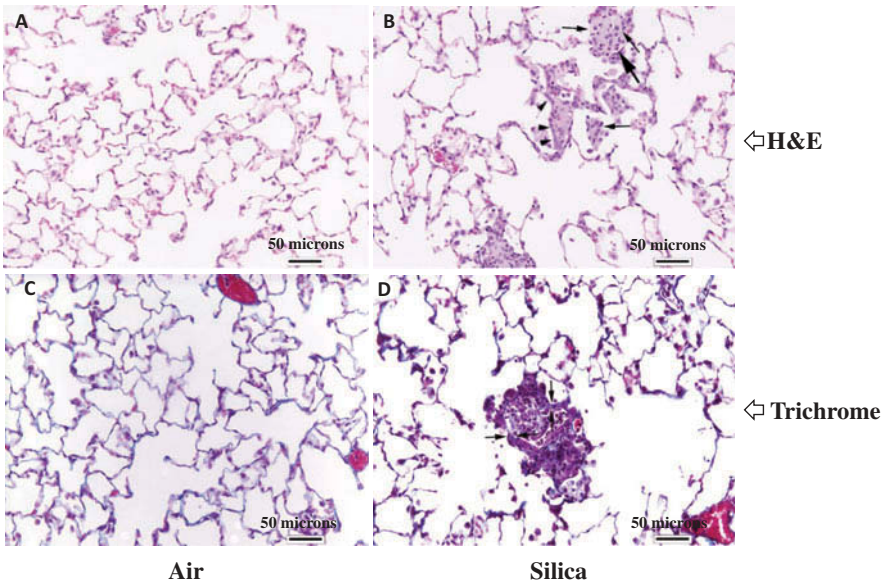

Figure 4. Photomicrographs of lung sections of rats. Lung sections of control and silica exposed rats were prepared and stained with H&E (A and B) or Mason's trichrome stain (C and D) as described under materials and methods section. In Figure B, the arrows indicate plump, alveolar macrophages with abundant, vacuolated cytoplasm and the arrowheads indicate plump, cuboidal type-II pneumocytes that typically line up along the alveolar area. Areas of thickened alveolar septa representing fibrosis are shown by arrows in the trichrome stained lung sections of the silica exposed rats (D). Magnification – 200X.

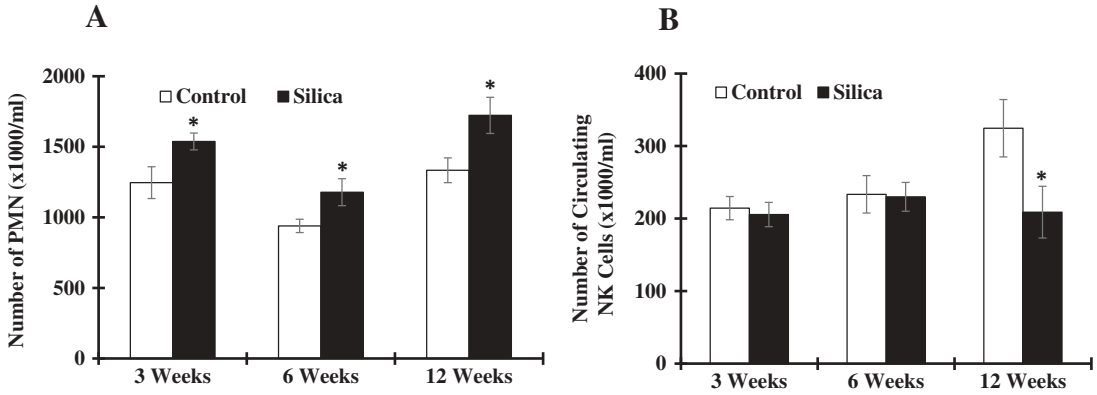

Figure 5. Hematological parameters in the rats. Various hematological parameters in the control and silica exposed rats were determined as described under the materials and methods section. Number of PMN (A) and NK cells (B) in the blood samples are presented. Values represent mean ± S.E. (n = 8).

*significantly different from time-matched controls ($p < 0.05$)

patients compared with matching controls (Subra et al. 2001).

Gene expression changes in rat lungs in response to crystalline silica exposure: Compared with corresponding controls, significant changes in global gene expression profiles were detected in lungs of all three groups of rats exposed to silica. The number of pulmonary SDEG found (38, 77, and 99 in the 3-, 6-, and 12-weeks group, respectively) corresponded to silica treatment dose and resulting tissue toxicity (Figure 6). The vast majority of the SDEG were overexpressed in the lungs in response to silica exposure. The expressions of 3, 13, and 34 genes were unique to 3-, 6-, and 12-month exposure groups, respectively (Figure 7). Among the SDEG detected, 32 genes were common in all three treatment groups (Table 2 and Figure 7). The fold changes in expression of many of the common SDEG were higher in the 6 and 12 weeks exposure groups compared with the 3 weeks animals (Table 2). The top 20 SDEG, expression fold changes, and FDR p values in each silica exposure group, compared to time-matched controls, is presented in Tables 3–5 and a complete list of the SDEG provided in Supplementary Table 2–4.

The gene expression alterations detected by microarray analysis were confirmed by results of QRT- PCR (Figure 8). In general, changes in gene expression for the SDEG were higher when determined by QRT-PCR compared to microarray. Similar observations were reported previously by Sellamuthu et al. (2011a), and this is attributed to

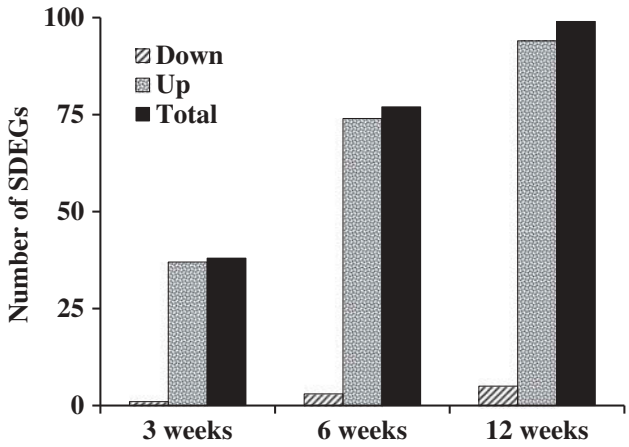

Figure 6. Number of significantly differentially expressed genes (SDEG) in the lungs of the silica exposed rats. Global gene expression profiles in the RNA samples isolated from the control and silica exposed rat lungs were determined by microarray analysis as described under materials and methods section. Number of SDEG (total, up-regulated and down-regulated) in the silica exposed rat lungs, compared with the corresponding time-matched controls, are presented. Values represent mean of 6 rats per group.

greater sensitivity and dynamic range offered by QRT-PCR platform, compared with the microarray platform, in detecting gene expression. The QRT-PCR results, in agreement with microarray data, further confirmed the correlation between total amount of silica deposited in lungs, resulting pulmonary toxicity, and alterations in gene expression.

Bioinformatic analysis of SDEG: Bioinformatic analysis of SDEG identified several biological function and canonical pathway categories that were

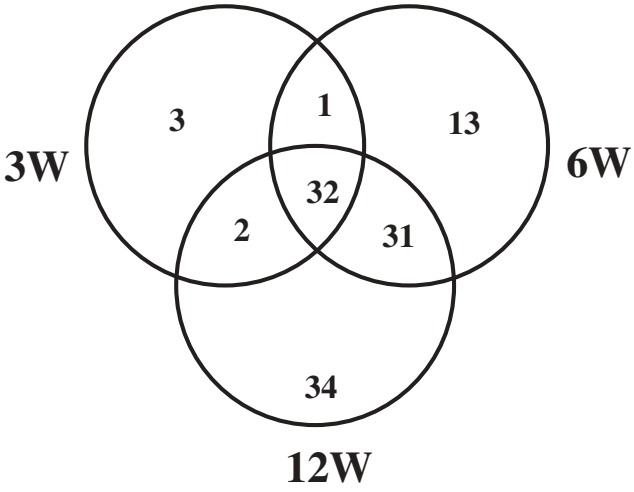

Figure 7. Venn diagram of significantly differentially expressed genes (SDEG) detected in the silica exposed rat lungs. The total number of SDEG detected in the lungs of the silica exposed rat lungs compared with the time-matched controls was determined by microarray analysis as descried under materials and methods section and used as input to prepare the Venn diagram. The number of SDGE unique to each of the exposure groups and common among the exposure groups are presented.

Table 2. Fold changes in expressions of genes significantly differentially expressed in the lung tissues of all three groups of rats exposed by inhalation to crystalline silica.

	Fold Changes in Expressions		
Gene Name (Gene Symbol)	3 W	6 W	12 W
ATPase H+ Transporting V0 Subunit D2 (ATP6VOD2)	1.63	1.71	1.69
B-cell leukemia/lymphoma 2 related protein A1d (BCL2A1D)	1.54	1.67	1.66
Complement component 4 binding protein, alpha (C4BPA)	1.97	2.37	2.61
Cd68 molecule (CD68)	1.63	1.76	1.64
Carcinoembryonic antigen-related cell adhesion molecule 10 (CEACAM10)	1.95	2.33	2.93
Chitinase 3 like 1 (CHI3L1)	1.95	2.05	2.47
Carbohydrate sulfotransferase 1 (CHST1)	1.65	2.07	1.79
Claudin 10 (CLDN10_Predicted)	1.75	1.83	1.76
C-X-C motif chemokine ligand 1 (CXCL1)	1.97	4.05	2.80
Fetuin B (FETUB)	1.60	1.89	1.86
Haptoglobin (HP)	1.54	1.73	1.89
Immunoglobulin superfamily, member 7 (IGSF7)	1.67	2.19	2.04
Lipocalin 2 (LCN2)	2.85	4.16	4.26
Placenta expressed transcript 1 (LOC363060/ Plet1)	1.53	1.67	1.63
Complement C3 (LOC497841/C3)	2.35	3.06	2.66
C2 calcium-dependent domain containing 4B (LOC501015/C2cd4b)	1.86	2.59	2.40
Lymphocyte antigen 6B (LY6B)	1.89	2.42	1.74
Matrix metallopeptidase 12 (MMP12)	3.33	2.68	2.22
Metallothionein 1a (MT1A)	1.73	1.75	1.92
NADPH oxidase organizer 1 (NOXO1_Predicted)	2.11	2.71	2.63
Nuclear receptor subfamily 1, group D, member 1 (NR1D1)	−3.23	−3.38	−3.17
PDZK1 interacting protein 1 (PDZK1IP1)	1.52	1.88	1.66
Platelet factor 4 (PF4)	1.70	2.03	1.71
Resistin like alpha (RETNLA)	2.46	2.60	4.39
CD177 antigen (RGD1562941_Predicted/ CD177)	4.66	6.30	5.18
Ribonuclease A family member 9 (RNASE9)	1.84	2.49	2.24
Solute carrier family 13 member 2 (SLC13A2)	1.60	1.88	1.85
Solute carrier family 16 (monocarboxylic acid transporters), member 11 (Predicted) (SLC16A11_Predicted)	1.50	1.66	1.59
Solute carrier family 26 member 4 (SLC26A4)	3.62	6.07	5.68
Solute carrier family 7 member 7 (SLC7A7)	1.52	1.71	1.85
Superoxide dismutase 2, mitochondrial (SOD2)	1.60	2.07	2.24
Triggering receptor expressed on myeloid cells 2 (TREM2_Predicted)	1.57	1.85	1.64

FDR p values for the SDEGs listed above can be found in Supplementary Table 2–4.

significantly enriched in response to crystalline silica exposure. Cancer, cell death and survival, cell-to-cell signaling and interaction, cellular growth and proliferation, cell movement, free radical scavenging, immune cell trafficking, inflammatory disease, inflammatory response, organismal injury and abnormalities, protein synthesis, and respiratory disease were among the prominent biological function categories that were significantly enriched (Figure 9). The canonical pathways that were significantly enriched in response to silica exposure in lungs included acute phase response signaling, agranulocyte adhesion and diapedesis, complement system, granulocyte adhesion and diapedesis, IL-10 signaling, and LXR/RXR activation (Figure 10). Similar to various pulmonary toxicity parameters determined, enrichment of each IPA biological function and canonical pathway category in the rats also corresponded to estimated amount of crystalline silica deposited in the rat lungs and resulting pulmonary toxicity. A molecular network consisting of 18 genes that were significantly different in all three groups of silica exposed rats, compared with time-matched controls, is presented in Figure 11. The central molecules in the network, including nuclear factor kappa B (NFkB), interleukin 1 (IL1), vascular endothelial growth factor (VEGF), platelet derived growth factor BB (PDGF BB), and low density lipoprotein (LDL), with which the SDEG interact, directly or indirectly, to form the network are known to be involved in inflammation and/or fibrosis - functions relevant to silica-induced pulmonary toxicity (Castronova 2004; Fan et al. 2013;

Table 3. Fold changes in expressions of the top 20 significantly differentially expressed genes (SDEGs) in the lung tissues of rats exposed by inhalation to crystalline silica for 3 weeks.

Gene Name (Gene Symbol)	Fold Change
CD177 antigen (RGD1562941_Predicted/CD177)	4.66
Solute carrier family 26 member 4 (SLC26A4)	3.62
Matrix metallopeptidase 12 (MMP12)	3.33
Lipocalin 2 (LCN2)	2.85
Resistin like alpha (RETNLA)	2.46
Complement C3 (LOC497841/C3)	2.35
NADPH oxidase organizer 1 (NOX01_Predicted)	2.11
C-X-C motif chemokine ligand 1 (CXCL1)	1.97
Complement component 4 binding protein, alpha (C4BPA)	1.97
Carcinoembryonic antigen-related cell adhesion molecule 10 (CEACAM10)	1.95
Chitinase 3 like 1 (CHI3L1)	1.95
Lymphocyte antigen 6B (LY6B)	1.89
C2 calcium-dependent domain containing 4B (LOC501015/C2cd4b)	1.86
Ribonuclease A family member 9 (RNASE9)	1.84
Claudin 10 (CLDN10_Predicted)	1.75
Metallothionein 1a (MT1A)	1.73
Platelet factor 4 (PF4)	1.70
C-C motif chemokine ligand 20 (CCL20)	1.69
Immunoglobulin superfamily, member 7 (IGSF7)	1.67
Carbohydrate sulfotransferase 1 (CHST1)	1.64

FDR p values of the SDEGs listed above and a complete list of all SDEGs detected in the rat lungs can be found in Supplementary Table 2.

Table 4. Fold changes in expressions of the top 20 significantly differentially expressed genes (SDEGs) in the lung tissues of rats exposed by inhalation to crystalline silica for 6 weeks.

Gene Name (Gene Symbol)	Fold Change
CD177 antigen (RGD1562941_Predicted/CD177)	6.30
Solute carrier family 26 member 4 (SLC26A4)	6.07
Lipocalin 2 (LCN2)	4.16
C-X-C motif chemokine ligand 1 (CXCL1)	4.05
Complement C3 (LOC497841/C3)	3.06
C-X-C Motif Chemokine Ligand 5 (CXCL5)	2.88
NADPH oxidase organizer 1 (NOXO1_Predicted)	2.71
Matrix metallopeptidase 12 (MMP12)	2.68
Resistin like alpha (RETNLA)	2.60
C2 calcium-dependent domain containing 4B (LOC501015/C2cd4b)	2.59
Ribonuclease A family member 9 (RNASE9)	2.49
Lymphocyte antigen 6B (LY6B)	2.42
Complement component 4 binding protein, alpha (C4BPA)	2.37
Carcinoembryonic antigen-related cell adhesion molecule 10 (CEACAM10)	2.33
Immunoglobulin superfamily, member 7 (IGSF7)	2.19
Carbohydrate sulfotransferase 1 (CHST1)	2.07
Superoxide dismutase 2, mitochondrial (SOD2)	2.07
Chitinase 3 like 1 (CHI3L1)	2.05
Platelet factor 4 (PF4)	2.03
Fetuin B (FETUB)	1.89

FDR p values of the SDEGs listed above and a complete list of all SDEGs detected in the rat lungs can be found in Supplementary Table 3.

Table 5. Fold changes in expressions of the top 20 significantly differentially expressed genes (SDEGs) in the lung tissues of rats exposed by inhalation to crystalline silica for 12 weeks.

Gene Name (Gene Symbol)	Fold Change
Solute carrier family 26 member 4 (SLC26A4)	5.68
CD177 antigen (Predicted) (RGD1562941_Predicted/CD177)	5.18
Resistin like alpha (RETNLA)	4.39
Lipocalin 2 (LCN2)	4.26
Secreted phosphoprotein 1 (SPP1)	3.51
Carcinoembryonic antigen-related cell adhesion molecule 10 (CEACAM10)	2.93
C-X-C motif chemokine ligand 1 (CXCL1)	2.80
Complement C3 (LOC497841/C3)	2.66
NADPH oxidase organizer 1 (Predicted) (NOXO1_Predicted)	2.63
Complement component 4 binding protein, alpha (C4BPA)	2.61
Chitinase 3 like 1 (CHI3L1)	2.47
C2 calcium-dependent domain containing 4B (LOC501015/C2cd4b)	2.40
Ribonuclease A family member 9 (RNASE9)	2.24
Superoxide dismutase 2, mitochondrial (SOD2)	2.23
Matrix metallopeptidase 12 (MMP12)	2.22
Immunoglobulin heavy chain 1a (Predicted) (IGH-1A_Predicted)	2.19
Immunoglobulin superfamily, member 7 (IGSF7)	2.04
C-X3-C motif chemokine ligand 1 (CX3CL1)	2.03
C-C motif chemokine ligand 2 (CCL2)	1.97
Metallothionein 1a (MT1A)	1.92

FDR p values of the SDEGs listed above and a complete list of all SDEGs detected in the rat lungs can be found in Supplementary Table 4.

Min, Cho, and Kwon 2012; Shaik-Dasthagirisaheb et al. 2013).

Discussion

Inhalation is the primary route for exposure to dust containing crystalline silica and lungs represent the major target organ for the resulting toxicity and adverse health effects. Workers employed in specific occupations such as mining, drilling, sand blasting, construction, and hydraulic fracturing are at an elevated risk for exposure to crystalline silica through dust inhalation. Recently, Pavilonis and Mirer (2017) reported that workers, especially drillers and dock builders, engaged in the World Trade Center clean-up operations were exposed to crystalline silica at levels significantly higher than the OSHA PEL and NIOSH REL. Similar excessive inhalation exposure to crystalline silica was noted previously among workers

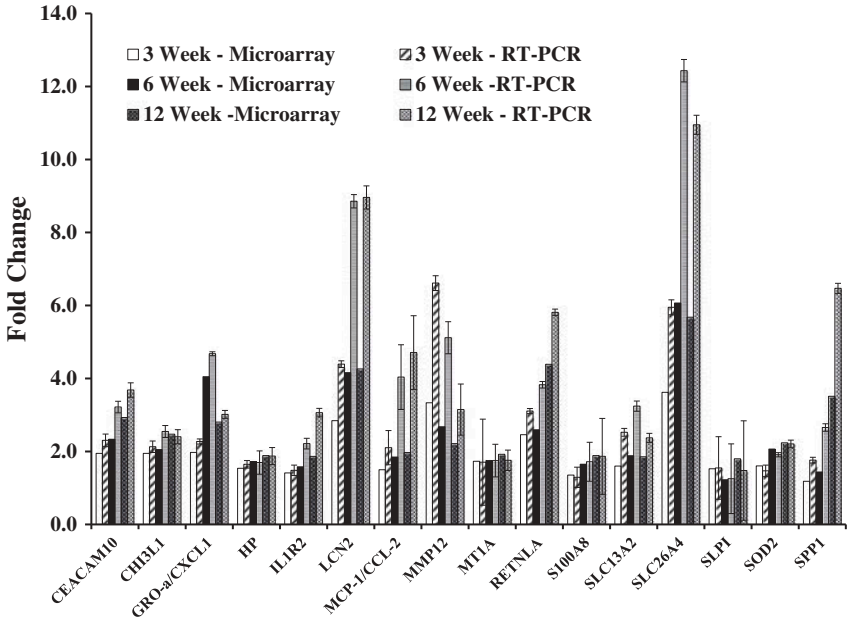

Figure 8. Real-time quantitative PCR confirmation of microarray data. PCR amplification and quantitation of a set of 16 genes were conducted as described under materials and methods section. PCR data represent the fold changes in the silica exposed rat lungs compared with the time-matched control rats. For comparison, the fold changes in expressions of the genes as determined by microarray analysis are also presented.

employed in hydraulic fracturing (Esswein et al. 2013). In the current study, the durations of inhalation exposures were adjusted to result in cumulative alveolar deposition of silica particles in the rat lungs that would correspond to exposure among workers within the REL (3 weeks) or higher (6 and 12 weeks).

Identification of the genes significantly differentially expressed in response to exposure to toxic agents and bioinformatic analysis of those genes

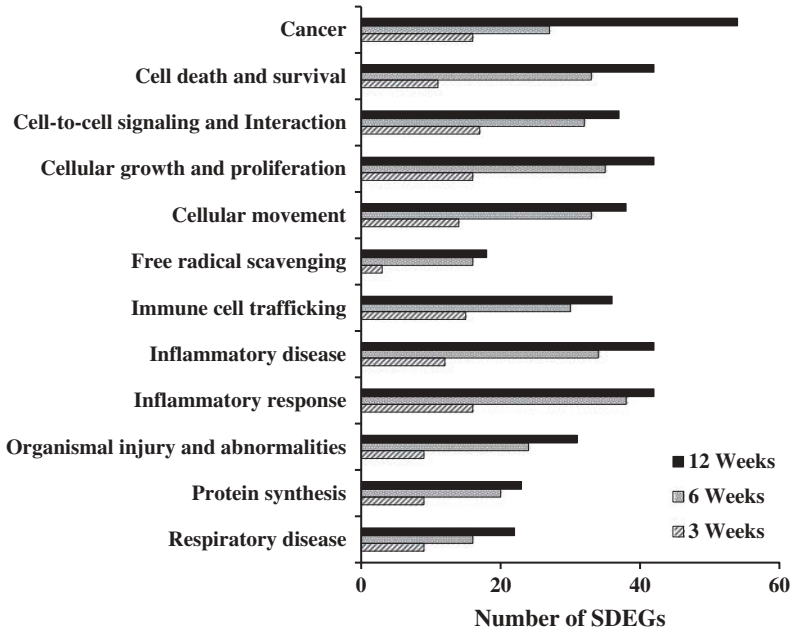

Figure 9. Enrichment of IPA biological functions in the lungs of the silica exposed rats. Ingenuity pathway analysis (IPA) software was employed to conduct bioinformatic analysis of the lung gene expression data of the rats as described under materials and methods section. A set of 12 IPA biological function categories significantly enriched in the lungs of the silica exposed rats, compared with the time-matched controls, are presented. Data represent the mean of 6 rats per group.

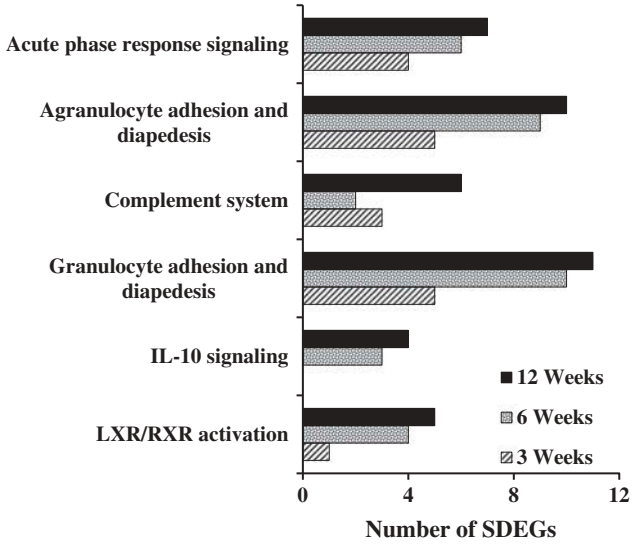

Figure 10. Enrichment of IPA canonical pathways in the lungs of the silica exposed rats. Ingenuity pathway analysis (IPA) software was employed to conduct bioinformatic analysis of the lung gene expression data of the rats as described under materials and methods section. A set of 6 IPA canonical pathway categories significantly enriched in the lungs of the silica exposed rats, compared with the time-matched controls, are presented. Data represent the mean of 6 rats per group.

offer unique advantages in toxicity studies. It is well established that gene expression changes exhibit enhanced sensitivity to detect toxicity compared with traditional histological and biochemical toxicity parameters (Heinloth et al. 2004; Umbright et al. 2010). This has enabled development of gene expression signatures, especially in easily available surrogate biospecimens such as blood, as sensitive biomarkers for detection of target organ toxicity (Bushel et al. 2007; Lobenhofer et al., 2008; Sellamuthu et al. 2011b). Similarly, bioinformatic analysis of gene expression data obtained from target organs and surrogate tissues provides insights into the mechanisms underlying target organ toxicity (Lobenhoffer et al., 2008; Sellamuthu et al. 2012, 2011b, 2013).

Crystalline silica particles, following inhalation, are phagocytosed by AM for detoxification and removal from lungs to prevent particle accumulation and ensuing pulmonary and/or systemic toxicity. However, interaction between inhaled silica particles and AM results in activation of macrophages. Activated macrophages release a variety of mediators such as reactive oxygen species (ROS), reactive nitrogen species (RNS), bioactive lipids, proteases, inflammatory cytokines, and pro-fibrotic factors that play critical roles in pulmonary toxicity (Laskin et al. 2011). The net result of release of these mediators by AM in response to the alveolar deposition of silica particles is induction of lung damage, inflammation, and fibrosis culminating in silicosis or other adverse health effects.

The interaction of inhaled silica particles with AM and alveolar epithelium results in the generation of highly reactive molecules, including ROS, which are known to play significant roles in the pathology associated with silica exposure (Porter et al. 2004). Results of bioinformatic analysis of the SDEG detected in rat lungs, in addition to supporting involvement of ROS in lung pathology, provided an understanding of the molecular mechanisms underlying the generation of ROS potentially resulting in oxidative stress and pulmonary toxicity in response to sub-chronic inhalation exposure to silica. The SDEG detected in silica treated rat lungs included both facilitators of ROS generation and responders to the resulting oxidative stress. The predicted transcript for *NOXO1* gene that was significantly overexpressed in all three silica groups codes the protein regulating the gene, NOX1, responsible for generation of

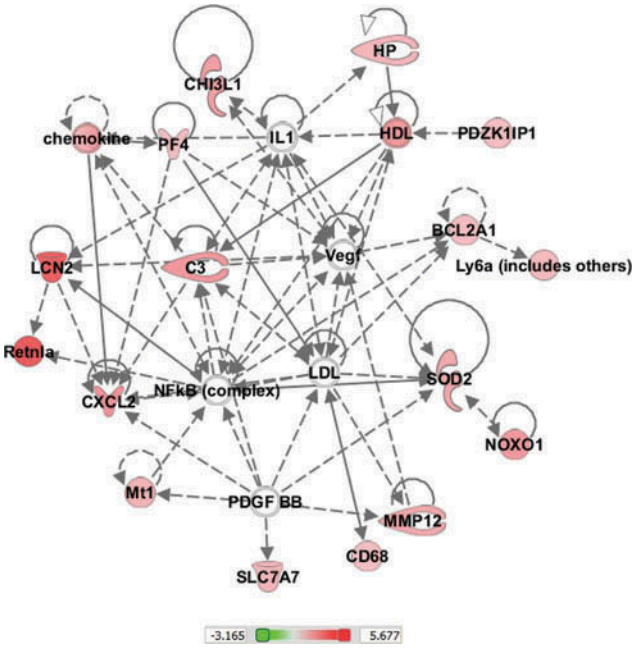

Figure 11. Enrichment of a molecular network in the silica exposed rat lungs. For clarity, only 18 common SDEG detected in the 3, 6, and 12 weeks of silica exposed rats and the molecules with which they directly and indirectly interact are shown in the network.

the highly reactive and, therefore, toxic superoxide anion (Yamamoto et al. 2013). The superoxide radical thus generated, under normal cellular conditions, is dismutated to another ROS, H_2O_2, by the catalytic activity of superoxide dismutases (Winterbourn and Metodiewa 1999). SOD2, a member of the superoxide dismutase family of genes was significantly overexpressed in lungs of all three treatment groups (Table 2).

The significant overexpression of *NOXO1* and *SOD2* genes in silica exposed rats suggested the potential for generation of ROS to induce oxidative stress and toxicity. This assumption is further strengthened by the observation that several genes known to be transcriptionally activated in response to oxidative stress were significantly overexpressed in lungs following silica treatment. These included metallothionein 1A (MT1A) (Chiaverini and De Ley 2010), heme oxygenase 1 (HMOX1) (Carosino et al. 2015; Joseph, He, and Umbright 2008), haptoglobin (HP) (Belcher et al. 2016), secreted phosphoprotein 1 (SPP1) (Schunke et al. 2013), lipocalin 2 (LCN2) (Alwahsh et al. 2014), and arginase 1 (ARG1) (Ogino et al. 2011). All these genes belonged to the IPA biological function category, free radical scavenging, which was found significantly enriched in lungs of all three silica exposed groups (Figure 9 and Supplementary Table 5, 7, and 9).

Induction of inflammation plays a significant role in silica-induced pulmonary toxicity and adverse health effects including silicosis (Castranova 2004). A significant elevation in the number of AM and PMN in the BAL as well as the lung histological changes observed in silica treated animals suggested induction of pulmonary inflammation in agreement with previous reports (Porter et al. 2004: Sellamuthu et al. 2011b). Results of bioinformatic analysis of gene expression data further supported silica-induced pulmonary inflammation in the rats. Inflammatory response, inflammatory disease, immune cell trafficking, and cellular movement were among some of the top ranked IPA biological functions that were significantly enriched in pulmonary tissue of particle treated rats (Figure 9 and Supplemental Table 5, 7, and 9). Similarly, a significant enrichment of the IPA canonical pathways acute phase response signaling (Shannahan et al. 2012), complement system (McGeer, Klegeris, and McGeer 2005), granulocyte and agranulocyte adhesion and diapedesis (Thomas et al. 2004), IL-10 signaling (Liao et al. 2016), and LXR/RXR activation (Archer et al. 2013; Ning et al. 2013) (Figure 10 and Supplementary Tables 6, 8, and 10) further supported involvement of inflammation in pulmonary toxicity mediated by silica.

The signaling molecules released by AM in response to their activation by inhaled silica particles include those that mediate an inflammatory response in lungs. Endogenous danger signals or alarmins are one such class of molecules released by activated AM that play a significant role in inflammation (Cantin et al. 1992; Eklund et al. 1991). The transcript for *S100A8*, an alarmin, was significantly overexpressed in pulmonary tissue of silica inhaled rats (Supplementary Tables 3 and 4). Innate immune receptors such as pattern recognition receptors (PRRs) are down-stream targets for *S100A8* (Chen and Nunez 2010) resulting in an inflammatory response, similar to that noted in lungs following silica treatment. Many of the inflammatory molecules released by activated AM are chemotactic in nature and might facilitate recruitment of pro-inflammatory cells into the lungs, the site of silica deposition. The two major classes of inflammatory chemokines are the C-C and C-X-C motif chemokines. Several members of the C-C and C-X-C motif chemokines, such as *CCl2, CXCL2, CXCL9, CXCL11, CXCL16, CXCL17* and *CX3CL1* were significantly overexpressed in pulmonary tissue of rats in response to sub-chronic inhalation exposure to silica (Supplementary Table 2–4). Platelet Factor 4 (PF4), another significantly overexpressed chemokine in lungs of silica treated rodents is a potent chemoattractant for neutrophils, monocytes and fibroblasts (Lasagni et al. 2003). Shi et al. (2013) demonstrated involvement of PF4 in the phenotypic changes in response to tissue injury including generation of inflammatory molecules. Similarly, the SLC26A4 gene whose transcript was highly overexpressed in all three silica groups (Table 2) is known to activate the C-X-C family of cytokines to facilitate neutrophil infiltration into lungs resulting in pulmonary inflammation (Nakao et al. 2008). The significant increase in number of AM and PMN detected in the BALF following

the silica treatment demonstrated the chemotactic response noted in the lungs of the rats in response to inhalation exposure (Figure 3). The significant accumulation of inflammatory cells in lungs and subsequent release of excess amounts of inflammatory mediators, such as cytokines, along with other toxic mediators such as ROS and RNS generated in response to crystalline silica exposure are key events that contributed to the ensuing pulmonary toxicity found in rats.

Silicosis, a serious adverse health effect resulting from excessive exposure to crystalline silica, is an obstructive pulmonary disease characterized by lung fibrosis. Pulmonary fibrosis, characteristic of silicosis, is a complex process resulting from excess deposition of collagen-rich extracellular matrix (ECM). Thickening of the lung epithelial septum in silica exposed rats as well as positive staining to Masson's trichrome stain suggested induction of fibrosis in pulmonary tissue (Figure 4). Significant changes in the expression of several genes that are known/likely to be involved in fibrosis were found in lungs of silica exposed rats. Matrix metalloproteinases (MMP) are a family of proteins that play critical roles in cell migration, leukocyte activation, fibroblast activation, collagen production, and chemokine processing - cellular processes related to fibrosis (Kang et al. 2007; Manicone and McGuire 2008; Parks, Wilson, and Lopez-Boado 2004). *MMP12*, a prominent pro-fibrotic member of the MMP family of genes (Kang et al. 2007; Madala et al. 2010; Matute-Bello et al. 2007), was highly overexpressed in lungs of all three silica treated groups (Table 2). The gene CHI3L1 codes the chitinase-3-like protein 1 whose overexpression in serum is considered a biomarker for pulmonary fibrosis (Furuhashi et al. 2010). By employing a transgenic mouse model, Kang et al. (2007) demonstrated that IL-18-induced pulmonary fibrosis is mediated via CHI3L1. *RETNLA1*, whose expression was significantly higher in treated lungs (Table 3) has multiple cellular functions including mitogenesis, angiogenesis and vascular remodeling (Angelini et al. 2009; Teng et al. 2003; Yamaji-Kegan et al. 2006). *RETNLA1* stimulates type 1 collagen and α-smooth muscle actin expression in lung fibroblasts indicative of myofibroblast differentiation, a key feature in lung fibrosis (Xu et al. 2012). *RETNLA1* is also induced in bleomycin-induced pulmonary fibrosis (Liu et al. 2014). Osteopontin, a glycoprotein encoded by the SPP1 gene is often considered a biomarker for pulmonary inflammation and/or fibrosis (Pardo et al. 2005). Compared to controls, *SPP1*, involved in extracellular matrix remodeling (O'Regan 2003), was highly overexpressed in the lungs of all three groups of silica exposed rats (Table 2). A significant overexpression of *SPP1*, as noted in the present study, was reported under conditions of asbestos-induced lung fibrosis (Sabo-Attwood et al., 2011). The overexpression of all these pulmonary genes (Table 2) and results of histological analysis showing fibrosis in the same lung samples (Figure 4) suggest involvement of these genes in the pulmonary fibrotic changes detected following sub-chronic inhalation exposure to crystalline silica.

The International Agency for Research on Cancer (IARC) has classified crystalline silica a 2A human carcinogen since there is sufficient evidence for its carcinogenicity in experimental animals and in humans (IARC 1997). Even though the carcinogenic aspect of crystalline silica was not currently investigated, data obtained in the present study supported previous findings that crystalline silica is a carcinogen (IARC 1997). Bioinformatic analysis of SDEG detected in lungs of silica exposed rats identified the IPA category, cancer, as one of the most significantly enriched biological function categories (Figure 9). The silica-induced oxidative stress may result in oxidative damage to DNA with potential to result in cancer (Kurfurstova et al. 2016; Peluso et al. 2015; Shi et al. 1998). A significant relationship is known to exist between inflammation and cancer (Todoric, Antonucci, and Karin 2016). Silicosis is mainly an inflammatory disease (Pollard 2016). Therefore, any of the mechanisms underlying silica-induced inflammation may be expected to contribute indirectly to the carcinogenic potential of crystalline silica.

Gene expression changes in response to exposure to a toxic agent, whether overexpression or down-regulation in expression, should not always be considered as an event leading to toxicity. Alternatively, gene expression changes may represent an adaptive response to detoxify the toxic agent to protect the biological system against

potential toxicity. Silica exposure is known to induce hemolysis (Pavan et al. 2014) which might result in the generation of free hemoglobin (Hb) (Olsson et al. 2012). Free Hb is a pro-oxidant and, therefore, needs to be detoxified to prevent its cellular accumulation potentially resulting in toxicity. The binding of Hb with haptoglobin (HP), catalyzed by heme oxygenase (HMOX), is an essential step involved in Hb detoxification (Alayash et al. 2013). In silica exposed rats, transcripts for both *HP* and *HMOX1* were significantly overexpressed (Supplementary Table 2–4) and this needs to be considered as an adaptive response by rat lungs to avert Hb-mediated pulmonary toxicity. Similarly, the release of cytokines and resulting chemotaxis of AM and PMN is primarily an adaptive response by rodents to detoxify and eliminate inhaled silica particles to prevent ensuing pulmonary toxicity found in this study. However, an uncontrolled or excessive release of chemokines and ensuing pulmonary accumulation of inflammatory cells and release of toxic intermediates may result in tissue injury. The observation that significant pulmonary toxicity, including fibrosis, was observed in rats suggested that such adaptive responses were overwhelmed following silica exposure. This is further supported by the observation that severity of silica-induced pulmonary toxicity in rats corresponded to the amount of crystalline silica that was estimated to be deposited in their lungs following inhalation exposure.

Various studies as well as those reported previously from our lab (Sellamuthu et al. 2011a, 2012, 2011b, 2013, 2017) contributed to understanding molecular mechanisms underlying silica-induced pulmonary toxicity. Previously, a rat model was employed where inhalation exposure to crystalline silica was conducted for one week (15 mg/m^3, 6 hr/day, 5 days/week) and pulmonary toxicity and gene expression profiles were determined at latency periods of 1–16 weeks (Sellamuthu et al. 2013), 32 weeks (Sellamuthu et al. 2011a), or 44 weeks (Sellamuthu et al., 2017). In the current investigation rats were exposed to the same concentration of silica, but for longer durations (3-, 6-, or 12-weeks) such that significantly higher cumulative exposure and alveolar deposition of crystalline silica occurred. Compared to the present study, where toxicity and gene expression profile were determined immediately following termination of inhalation exposure, the severity of pulmonary toxicity as well as number of SDEG and their expression level changes were higher as opposed to when the latency period following inhalation exposure to silica was longer (Sellamuthu et al. 2012, 2013, 2017). These findings suggest that post-exposure latency period, as expected from the progressive nature of silicosis, may be more important than the cumulative dose of silica exposure with respect to severity of pulmonary toxicity. In spite of these differences, a reliable similarity was found between the two groups of silica exposed rats (one-week exposure followed by varying latency periods vs. sub-chronic exposure of 3, 6, or 12 weeks with no latency periods) with respect to the SDEG detected and biological functions and canonical pathways that were significantly enriched in their lungs.

A large number of SDEG were detected in lungs of rats in response to inhalation exposure to crystalline silica in this study as well as those published previously from our lab (Sellamuthu et al. 2011a, 2012, 2013, 2017). Bioinformatic analysis of SDEG and interpretation of findings suggested involvement of many of the SDEG identified and pathways/networks mediated by those genes in silica-induced pulmonary toxicity. However, the precise role of any of the SDEG in the silica-mediated pulmonary toxicity remains to be determined. This will require future studies involving transgenic models (*in vitro* cell culture and/or *in vivo* animal models) for the individual SDEG and investigating silica-induced pulmonary toxicity in such models. In addition, pharmacological agents capable of blocking the function of the protein coded by the SDEG may be helpful in such studies determining the precise role of the SDEG in silica-induced pulmonary toxicity.

Disclaimer

The findings and conclusions in this report are those of the authors and do not necessarily represent the views of NIOSH.

The microarray data have been deposited in the Gene Expression Omnibus Database, http://www.ncbi.nlm.nih.gov/geo (accession number GSE49114).

References

Alayash, A. I., C. B. Andersen, S. K. Moestrup, and L. Bulow. 2013. Haptoglobin: The hemoglobin detoxifier in plasma. *Trends in Biotechnology* 31:2–3. doi:10.1016/j.tibtech.2012.10.003.

Alwahsh, S. M., M. Xu, H. A. Seyhan, S. Ahmad, S. Mihm, G. Ramadori, and F. C. Schultze. 2014. Diet high in fructose leads to an overexpression of lipocalin-2 in rat fatty liver. *World Journal of Gastroenterology : WJG* 20:1807–1821. doi:10.3748/wjg.v20.i7.1807.

Angelini, D. J., Q. Su, K. Yamaji-Kegan, C. Fan, J. T. Skinner, H. C. Champion, M. T. Crow, and R. A. Johns. 2009. Hypoxia-induced mitogenic factor (HIMF/FIZZ1/RELMalpha) induces the vascular and hemodynamic changes of pulmonary hypertension. *American Journal Physiological Lung Cellular Molecular Physiological* 296: L582–L593. doi:10.1152/ajplung.90526.2008.

Antonini, J. M., and J. R. Roberts. 2007. Chromium in stainless steel welding fume suppresses lung defense responses against bacterial infection in rats. *Journal Immunotoxicol* 4:117–127. doi:10.1080/15476910701336953.

Archer, A., E. Stolarczyk, M. L. Doria, L. Helguero, R. Domingues, J. K. Howard, A. Mode, M. Korach-Andre, and J. A. Gustafsson. 2013. LXR activation by GW3965 alters fat tissue distribution and adipose tissue inflammation in ob/ob female mice. *Journal of Lipid Research* 54:1300–1311. doi:10.1194/jlr.M033977.

Belcher, J. D., C. Chen, J. Nguyen, P. Zhang, F. Abdulla, P. Nguyen, T. Killeen, P. Xu, G. O'Sullivan, K. A. Nath, and G. M. Vercellotti. 2016. Control of oxidative stress and inflammation in sickle cell disease with the Nrf2 activator dimethyl fumarate. *Antioxidants & Redox Signaling* 26:748–762. doi:10.1089/ars.2015.6571.

Benjamini, Y., and Y. Hochberg. 1995. Controlling the false discovery rate: A practical and powerful approach to multiple testing. *Journal Roy Statistical Social Series* 57:289–300.

Brazma, A., P. Hingamp, J. Quackenbush, G. Sherlock, P. Spellman, C. Stoeckert, J. Aach, W. Ansorge, C. A. Ball, H. C. Causton, T. Gaasterland, P. Glenisson, F. C. Holstege, I. F. Kim, V. Markowitz, J. C. Matese, H. Parkinson, A. Robinson, U. Sarkans, S. Schulze-Kremer, J. Stewart, R. Taylor, J. Vilo, and M. Vingron. 2001. Minimum information about a microarray experiment (MIAME)-toward standards for microarray data. *Nature Genetics* 29:365–371. doi:10.1038/ng1201-365.

Bushel, P. R., A. N. Heinloth, J. Li, L. Huang, J. W. Chou, G. A. Boorman, D. E. Malarkey, C. D. Houle, S. M. Ward, R. E. Wilson, R. D. Fannin, M. W. Russo, P. B. Watkins, R. W. Tennant, and R. S. Paules. 2007. Blood gene expression signatures predict exposure levels. *Proceedings Natural Academic Sciences USA* 104:18211–18216. doi:10.1073/pnas.0706987104.

Cantin, A. M., P. Larivee, M. Martel, and R. Begin. 1992. Hyaluronan (hyaluronic acid) in lung lavage of asbestos-exposed humans and sheep. *Lung* 170:211–220. doi:10.1007/BF00174118.

Carosino, C. M., K. J. Bein, L. E. Plummer, A. R. Castaneda, Y. Zhao, A. S. Wexler, and K. E. Pinkerton. 2015. Allergic airway inflammation is differentially exacerbated by daytime and nighttime ultrafine and submicron fine ambient particles: Heme oxygenase-1 as an indicator of PM-mediated allergic inflammation. *Journal of Toxicology and Environmental Health. Part A* 78:254–266. doi:10.1080/15287394.2014.959627.

Castranova, V. 2004. Signaling pathways controlling the production of inflammatory mediators in response to crystalline silica exposure: Role of reactive oxygen/nitrogen species. *Free Radical Biology & Medicine* 37:916–925. doi:10.1016/j.freeradbiomed.2004.05.032.

Chen, B. T., D. Schwegler-Berry, W. McKinney, S. Stone, J. L. Cumpston, S. Friend, D. W. Porter, V. Castranova, and D. G. Frazer. 2012. Multi-walled carbon nanotubes: Sampling criteria and aerosol characterization. *Inhal Toxicogical* 24:798–820. doi:10.3109/08958378.2012.720741.

Chen, G. Y., and G. Nunez. 2010. Sterile inflammation: Sensing and reacting to damage. *Nature Reviews. Immunology* 10:826–837. doi:10.1038/nri2873.

Chiaverini, N., and M. De Ley. 2010. Protective effect of metallothionein on oxidative stress-induced DNA damage. *FreeRadical Research* 44:605–613. doi:10.3109/10715761003692511.

Cooper, G. S., F. W. Miller, and D. R. Germolec. 2002. Occupational exposures and autoimmune diseases. *International Immunopharmacology* 2:303–313. doi:10.1016/S1567-5769(01)00181-3.

Eklund, A., G. Tornling, E. Blaschke, and T. Curstedt. 1991. Extracellular matrix components in bronchoalveolar lavage fluid in quartz exposed rats. *British Journal Industrial Medica* 48:776–782.

Esswein, E. J., M. Breitenstein, J. Snawder, M. Kiefer, and W. K. Sieber. 2013. Occupational exposures to respirable crystalline silica during hydraulic fracturing. *Journal Occupational Environment Hygiene* 10:347–356. doi:10.1080/15459624.2013.788352.

Fan, B., L. Ma, Q. Li, L. Wang, J. Zhou, and J. Wu. 2013. Correlation between platelet-derived growth factor signaling pathway and inflammation in desoxycorticosterone-induced salt-sensitive hypertensive rats with myocardial fibrosis. *International Journal Clinical Experiments Pathologists* 6:2468–2475.

Furuhashi, K., T. Suda, Y. Nakamura, N. Inui, D. Hashimoto, S. Miwa, H. Hayakawa, H. Kusagaya, Y. Nakano, H. Nakamura, and K. Chida. 2010. Increased expression of YKL-40, a chitinase-like protein, in serum and lung of patients with idiopathic pulmonary fibrosis. *Respiratory Medica* 104:1204–1210. doi:10.1016/j.rmed.2010.02.026.

Gentleman, R. C., V. J. Carey, D. M. Bates, B. Bolstad, M. Dettling, S. Dudoit, B. Ellis, L. Gautier, Y. Ge, J. Gentry, K. Hornik, T. Hothorn, W. Huber, S. Iacus, R. Irizarry, F. Leisch, C. Li, M. Maechler, A. J. Rossini, G. Sawitzki, C. Smith, G. Smyth, L. Tierney, J. Y. Yang, and J. Zhang. 2004. Bioconductor: Open software development for

computational biology and bioinformatics. *Genome Biology* 5:R80. doi:10.1186/gb-2004-5-10-r80.

Gulumian, M., P. J. Borm, V. Vallyathan, V. Castranova, K. Donaldson, G. Nelson, and J. Murray. 2006. Mechanistically identified suitable biomarkers of exposure, effect, and susceptibility for silicosis and coal-worker's pneumoconiosis: A comprehensive review. *Journal Toxicogical Environment Health B* 9:357–395. doi:10.1080/15287390500196537.

Guo, N. L., Y. W. Wan, J. Denvir, D. W. Porter, M. Pacurari, M. G. Wolfarth, V. Castranova, and Y. Qian. 2012. Multiwalled carbon nanotube-induced gene signatures in the mouse lung: Potential predictive value for human lung cancer risk and prognosis. *Journal of Toxicology and Environmental Health. Part A* 75:1129–1153. doi:10.1080/15287394.2012.699852.

Heinloth, A. N., R. D. Irwin, G. A. Boorman, P. Nettesheim, R. D. Fannin, S. O. Sieber, M. L. Snell, C. J. Tucker, L. Li, G. S. Travlos, G. Vansant, P. E. Blackshear, R. W. Tennant, M. L. Cunningham, and R. S. Paules. 2004. Gene expression profiling of rat livers reveals indicators of potential adverse effects. *Toxicological Sciences : an Official Journal of the Society of Toxicology* 80:193–202. doi:10.1093/toxsci/kfh145.

Hnizdo, E., and V. Vallyathan. 2003. Chronic obstructive pulmonary disease due to occupational exposure to silica dust: A review of epidemiological and pathological evidence. *Occupational Environment Medica* 60:237–243. doi:10.1136/oem.60.4.237.

Huang, Y. C. 2013. The role of in vitro gene expression profiling in particulate matter health research. *Journal Toxicogical Environment Health B* 16:381–394. doi:10.1080/10937404.2013.832649.

IARC (International Agency for Research on Cancer). 1997. *IARC monographs on the evaluation of carcinogenic risk to humans: Silica, some silicates, coal dust and para-aramid fibrils*, vol. 68. Lyon, France: World halth Organization, International Agency for Resaerch on Cancer.

Ihaka, R., and R. Gentleman. 1996. R: A language for data analysis and graphics. *Journal Computation Graph Statistical* 5:299–314.

Joseph, P., Q. He, and C. Umbright. 2008. Heme-oxygenase 1 gene expression is a marker for hexavalent chromium-induced stress and toxicity in human dermal fibroblasts. *Toxicological Sciences : An Official Journal of the Society of Toxicology* 103:325–334. doi:10.1093/toxsci/kfn048.

Kang, H. R., S. J. Cho, C. G. Lee, R. J. Homer, and J. A. Elias. 2007. Transforming growth factor (TGF)-beta1 stimulates pulmonary fibrosis and inflammation via a Bax-dependent, bid-activated pathway that involves matrix metalloproteinase-12. *The Journal of Biological Chemistry* 282:7723–7732. doi:10.1074/jbc.M610764200.

Klaper, R., D. Arndt, J. Bozich, and G. Dominguez. 2014. Molecular interactions of nanomaterials and organisms: Defining biomarkers for toxicity and high-throughput screening using traditional and next-generation sequencing approaches. *Analyst* 139:882–895. doi:10.1039/C3AN01644G.

Kurfurstova, D., J. Bartkova, R. Vrtel, A. Mickova, A. Burdova, D. Majera, M. Mistrik, M. Kral, F. R. Santer, J. Bouchal, and J. Bartek. 2016. DNA damage signalling barrier, oxidative stress and treatment-relevant DNA repair factor alterations during progression of human prostate cancer. *Molecular Oncology* 10:879–894. doi:10.1016/j.molonc.2016.02.005.

Lasagni, L., M. Francalanci, F. Annunziato, E. Lazzeri, S. Giannini, L. Cosmi, C. Sagrinati, B. Mazzinghi, C. Orlando, E. Maggi, F. Marra, S. Romagnani, M. Serio, and P. Romagnani. 2003. An alternatively spliced variant of CXCR3 mediates the inhibition of endothelial cell growth induced by IP-10, Mig, and I-TAC, and acts as functional receptor for platelet factor 4. *The Journal of Experimental Medicine* 197:1537–1549. doi:10.1084/jem.20021897.

Laskin, D. L., V. R. Sunil, C. R. Gardner, and J. D. Laskin. 2011. Macrophages and tissue injury: Agents of defense or destruction? *Annual Review of Pharmacology and Toxicology* 51:267–288. doi:10.1146/annurev.pharmtox.010909.105812.

Leung, C. C., I. T. Yu, and W. Chen. 2012. Silicosis. *Lancet* 379:2008–2018. doi:10.1016/S0140-6736(12)60235-9.

Liao, C. T., M. Rosas, L. C. Davies, P. J. Giles, V. J. Tyrrell, V. B. O'Donnell, N. Topley, I. R. Humphreys, D. J. Fraser, S. A. Jones, and P. R. Taylor. 2016. IL-10 differentially controls the infiltration of inflammatory macrophages and antigen-presenting cells during inflammation. *European Journal of Immunology* 46:2222–2232. doi:10.1002/eji.201646528.

Liu, T., H. Yu, M. Ullenbruch, H. Jin, T. Ito, Z. Wu, J. Liu, and S. H. Phan. 2014. The in vivo fibrotic role of FIZZ1 in pulmonary fibrosis. *PLoS One* 9:e88362. doi:10.1371/journal.pone.0088362.

Lobenhofer, E. K., J. T. Auman, P. E. Blackshear, G. A. Boorman, P. R. Bushel, M. L. Cunningham, J. M. Fostel, K. Gerrish, A. N. Heinloth, R. D. Irwin, D. E. Malarkey, B. A. Merrick, S. O. Sieber, C. J. Tucker, S. M. Ward, R. E. Wilson, P. Hurban, R. W. Tennant, and R. S. Paules. 2008. Gene expression response in target organ and whole blood varies as a function of target organ injury phenotype. *Genome Biology* 9:R100. doi:10.1186/gb-2008-9-6-r100.

Madala, S. K., J. T. Pesce, T. R. Ramalingam, M. S. Wilson, S. Minnicozzi, A. W. Cheever, R. W. Thompson, M. M. Mentink-Kane, and T. A. Wynn. 2010. Matrix metalloproteinase 12-deficiency augments extracellular matrix degrading metalloproteinases and attenuates IL-13-dependent fibrosis. *Journal of Immunology (Baltimore, Md. : 1950)* 184:3955–3963. doi:10.4049/jimmunol.0903008.

Madl, A. K., E. P. Donovan, S. H. Gaffney, M. A. McKinley, E. C. Moody, J. L. Henshaw, and D. J. Paustenbach. 2008. State-of-the-science review of the occupational health hazards of crystalline silica in abrasive blasting operations and related requirements for respiratory protection.

Journal Toxicogical Environment Health B 1:548–608. doi:10.1080/10937400801909135.

Manicone, A. M., and J. K. McGuire. 2008. Matrix metalloproteinases as modulators of inflammation. *Seminars in Cell & Developmental Biology* 19:34–41. doi:10.1016/j.semcdb.2007.07.003.

Matute-Bello, G., M. M. Wurfel, J. S. Lee, D. R. Park, C. W. Frevert, D. K. Madtes, S. D. Shapiro, and T. R. Martin. 2007. Essential role of MMP-12 in Fas-induced lung fibrosis. *American JRespir Cellular Molecular Biologic* 37:210–221. doi:10.1165/rcmb.2006-0471OC.

Mazurek, J. M., P. L. Schleiff, J. M. Wood, S. A. Hendricks, and A. Weston; Control Centers for Disease, and Prevention. 2015. Notes from the field: Update: Silicosis mortality - United States, 1999–2013. *Morb Mortal Wkly Reports* 64:653–654.

McGeer, E. G., A. Klegeris, and P. L. McGeer. 2005. Inflammation, the complement system and the diseases of aging. *Neurobiology of Aging* 26 (Suppl 1):94–97. doi:10.1016/j.neurobiolaging.2005.08.008.

McKinney, W., B. Chen, and D. Frazer. 2009. Computer controlled multi-walled carbon nanotube inhalation exposure system. *Inhal Toxicogical* 21:1053–1061. doi:10.1080/08958370802712713.

Min, K. J., K. H. Cho, and T. K. Kwon. 2012. The effect of oxidized low density lipoprotein (oxLDL)-induced heme oxygenase-1 on LPS-induced inflammation in RAW 264.7 macrophage cells. *Cellular Signalling* 24:1215–1221. doi:10.1016/j.cellsig.2012.02.001.

Nakao, I., S. Kanaji, S. Ohta, H. Matsushita, K. Arima, N. Yuyama, M. Yamaya, K. Nakayama, H. Kubo, M. Watanabe, H. Sagara, K. Sugiyama, H. Tanaka, S. Toda, H. Hayashi, H. Inoue, T. Hoshino, A. Shiraki, M. Inoue, K. Suzuki, H. Aizawa, S. Okinami, H. Nagai, M. Hasegawa, T. Fukuda, E. D. Green, and K. Izuhara. 2008. Identification of pendrin as a common mediator for mucus production in bronchial asthma and chronic obstructive pulmonary disease. *Journal of Immunology (Baltimore, Md. : 1950)* 180:6262–6269. doi:10.4049/jimmunol.180.9.6262.

Ning, R. B., J. Zhu, D. J. Chai, C. S. Xu, H. Xie, X. Y. Lin, J. Z. Zeng, and J. X. Lin. 2013. RXR agonists inhibit high glucose-induced upregulation of inflammation by suppressing activation of the NADPH oxidase-nuclear factor-kappaB pathway in human endothelial cells. *Genetics and Molecular Research : GMR* 12:6692–6707. doi:10.4238/2013.December.13.3.

NIOSH (National Institute for Occupational Safety and Health). 2002. Hazard review: Health effects of occupational exposures to respirable crystalline silica. US Department of Health and Human Services (NIOSH) Publication No. 2002-129. Available from: http://www.cdc.gov/niosh/docs/2002-129/02-129a.html.

O'Regan, A. 2003. The role of osteopontin in lung disease. *Cytokine & Growth Factor Reviews* 14:479–488. doi:10.1016/S1359-6101(03)00055-8.

Ogino, K., N. Takahashi, T. Takigawa, Y. Obase, and D. H. Wang. 2011. Association of serum arginase I with oxidative stress in a healthy population. *FreeRadical Research* 45:147–155. doi:10.3109/10715762.2010.520318.

Olsson, M. G., M. Allhorn, L. Bulow, S. R. Hansson, D. Ley, M. L. Olsson, A. Schmidtchen, and B. Akerstrom. 2012. Pathological conditions involving extracellular hemoglobin: Molecular mechanisms, clinical significance, and novel therapeutic opportunities for alpha(1)-microglobulin. *Antioxidants Redox Signalling* 17:813–846. doi:10.1089/ars.2011.4282.

OSHA (Occupational Safety and Health Administration). 2016. Occupational exposure to crystalline silica: Final rule. Available from: www.federal register.gov/articles/2016/03/25/2016-04800/2016-04800/occupational-exposure-to-crystalline-silica.

Pardo, A., K. Gibson, J. Cisneros, T. J. Richards, Y. Yang, C. Becerril, S. Yousem, I. Herrera, V. Ruiz, M. Selman, and N. Kaminski. 2005. Up-regulation and profibrotic role of osteopontin in human idiopathic pulmonary fibrosis. *PLoS Medicine* 2:e251. doi:10.1371/journal.pmed.0020251.

Parks, W. C., C. L. Wilson, and Y. S. Lopez-Boado. 2004. Matrix metalloproteinases as modulators of inflammation and innate immunity. *Nature Reviews. Immunology* 4:617–629. doi:10.1038/nri1418.

Pavan, C., V. Rabolli, M. Tomatis, B. Fubini, and D. Lison. 2014. Why does the hemolytic activity of silica predict its pro-inflammatory activity? *Particle Fibre Toxicogical* 11:76. doi:10.1186/s12989-014-0076-y.

Pavilonis, B. T., and F. E. Mirer. 2017. Respirable dust and silica exposure among world trade center cleanup workers. *Journal Occupational Environment Hygiene* 14:187–194. doi:10.1080/15459624.2016.1237773.

Peluso, M. E., A. Munnia, R. W. Giese, E. Chellini, M. Ceppi, and F. Capacci. 2015. Oxidatively damaged DNA in the nasal epithelium of workers occupationally exposed to silica dust in Tuscany region, Italy. *Mutagenesis* 30:519–525. doi:10.1093/mutage/gev014.

Pollard, K. M. 2016. Silica, silicosis, and autoimmunity. *Frontiers Immunology* 7:97. doi:10.3389/fimmu.2016.00097.

Porter, D. W., A. F. Hubbs, R. Mercer, V. A. Robinson, D. Ramsey, J. McLaurin, A. Khan, L. Battelli, K. Brumbaugh, A. Teass, and V. Castranova. 2004. Progression of lung inflammation and damage in rats after cessation of silica inhalation. *Toxicological Sciences : An Official Journal of the Society of Toxicology* 79:370–380. doi:10.1093/toxsci/kfh110.

Porter, D. W., D. Ramsey, A. F. Hubbs, L. Battelli, J. Ma, M. Barger, D. Landsittel, V. A. Robinson, J. McLaurin, A. Khan, W. Jones, A. Teass, and V. Castranova. 2001. Time course of pulmonary response of rats to inhalation of crystalline silica: Histological results and biochemical indices of damage, lipidosis, and fibrosis. *Journal of Environmental Pathology, Toxicology and Oncology* 20 (Suppl 1):1–14. doi:10.1615/JEnvironPatholToxicolOncol.v20.iSuppl.1.

Rees, D., and J. Murray. 2007. Silica, silicosis and tuberculosis. *The International Journal of Tuberculosis and Lung Disease* 11:474–484.

Sabo-Attwood, T., M. E. Ramos-Nino, M. Eugenia-Ariza, M. B. Macpherson, K. J. Butnor, P. C. Vacek, S. P. McGee, J. C. Clark, C. Steele, and B. T. Mossman. 2011. Osteopontin modulates inflammation, mucin production, and gene expression signatures after inhalation of asbestos in a murine model of fibrosis. *The American Journal of Pathology* 178:1975–1985. doi:10.1016/j.ajpath.2011.01.048.

Schunke, K. J., L. Coyle, G. F. Merrill, and D. T. Denhardt. 2013. Acetaminophen attenuates doxorubicin-induced cardiac fibrosis via osteopontin and GATA4 regulation: Reduction of oxidant levels. *Journal Cellular Physiological* 228:2006–2014. doi:10.1002/jcp.24367.

Sellamuthu, R., C. Umbright, S. Li, M. Kashon, and P. Joseph. 2011a. Mechanisms of crystalline silica-induced pulmonary toxicity revealed by global gene expression profiling. *Inhal Toxicogical* 23:927–937.

Sellamuthu, R., C. Umbright, J. R. Roberts, R. Chapman, S. H. Young, D. Richardson, J. Cumpston, W. McKinney, B. T. Chen, D. Frazer, S. Li, M. Kashon, and P. Joseph. 2012. Transcriptomics analysis of lungs and peripheral blood of crystalline silica-exposed rats. *Inhal Toxicogical* 24:570–579. doi:10.3109/08958378.2012.697926.

Sellamuthu, R., C. Umbright, J. R. Roberts, R. Chapman, S. H. Young, D. Richardson, H. Leonard, W. McKinney, B. Chen, D. Frazer, S. Li, M. Kashon, and P. Joseph. 2011b. Blood gene expression profiling detects silica exposure and toxicity. *Toxicological Sciences : An Official Journal of the Society of Toxicology* 122:253–264. doi:10.1093/toxsci/kfr125.

Sellamuthu, R., C. Umbright, J. R. Roberts, A. Cumpston, W. McKinney, B. T. Chen, D. Frazer, S. Li, M. Kashon, and P. Joseph. 2013. Molecular insights into the progression of crystalline silica-induced pulmonary toxicity in rats. *Journal Applications Toxicogical* 33:301–312. doi:10.1002/jat.v33.4.

Sellamuthu, R., C. Umbright, J. R. Roberts, S. H. Young, D. Richardson, W. McKinney, B. T. Chen, S. Li, M. Kashon, and P. Joseph. 2017. Molecular mechanisms of pulmonary response progression in crystalline silica exposed rats. *Inhal Toxicogical* 29:53–64. doi:10.1080/08958378.2017.1282064.

Shaik-Dasthagirisaheb, Y. B., G. Varvara, G. Murmura, A. Saggini, G. Potalivo, A. Caraffa, P. Antinolfi, S. Tete, D. Tripodi, F. Conti, E. Cianchetti, E. Toniato, M. Rosati, P. Conti, L. Speranza, A. Pantalone, R. Saggini, T. C. Theoharides, and F. Pandolfi. 2013. Vascular endothelial growth factor (VEGF), mast cells and inflammation. *International Journal Immunopathol Pharmacology* 26:327–335. doi:10.1177/039463201302600206.

Shannahan, J. H., O. Alzate, W. M. Winnik, D. Andrews, M. C. Schladweiler, A. J. Ghio, S. H. Gavett, and U. P. Kodavanti. 2012. Acute phase response, inflammation and metabolic syndrome biomarkers of Libby asbestos exposure. *Toxicology and Applied Pharmacology* 260:105–114. doi:10.1016/j.taap.2012.02.006.

Shi, G., D. J. Field, X. Long, D. Mickelsen, K. A. Ko, S. Ture, V. A. Korshunov, J. M. Miano, and C. N. Morrell. 2013. Platelet factor 4 mediates vascular smooth muscle cell injury responses. *Blood* 121:4417–4427. doi:10.1182/blood-2012-09-454710.

Shi, X., V. Castranova, B. Halliwell, and V. Vallyathan. 1998. Reactive oxygen species and silica-induced carcinogenesis. *Journal Toxicogical Environment Health B* 1:181–197. doi:10.1080/10937409809524551.

Steenland, K., and D. F. Goldsmith. 1995. Silica exposure and autoimmune diseases. *American Journal of Industrial Medicine* 28:603–608. doi:10.1002/(ISSN)1097-0274.

Subra, J. F., G. Renier, P. Reboul, F. Tollis, R. Boivinet, P. Schwartz, and A. Chevailler. 2001. Lymphopenia in occupational pulmonary silicosis with or without autoimmune disease. *Clinical and Experimental Immunology* 126:540–544. doi:10.1046/j.1365-2249.2001.01696.x.

Teng, X., D. Li, H. C. Champion, and R. A. Johns. 2003. FIZZ1/RELMalpha, a novel hypoxia-induced mitogenic factor in lung with vasoconstrictive and angiogenic properties. *Circulation Research* 92:1065–1067. doi:10.1161/01.RES.0000073999.07698.33.

Thomas, R. M., C. Schmedt, M. Novelli, B. K. Choi, J. Skok, A. Tarakhovsky, and J. Roes. 2004. C-terminal SRC kinase controls acute inflammation and granulocyte adhesion. *Immunity* 20:181–191. doi:10.1016/S1074-7613(04)00023-8.

Todoric, J., L. Antonucci, and M. Karin. 2016. Targeting inflammation in cancer prevention and therapy. *Cancer Prevention Researcher* 9:895–905. doi:10.1158/1940-6207.CAPR-16-0209.

Umbright, C., R. Sellamuthu, S. Li, M. Kashon, M. Luster, and P. Joseph. 2010. Blood gene expression markers to detect and distinguish target organ toxicity. *Molecular and Cellular Biochemistry* 335:223–234. doi:10.1007/s11010-009-0272-5.

Vupputuri, S., C. G. Parks, L. A. Nylander-French, A. Owen-Smith, S. L. Hogan, and D. P. Sandler. 2012. Occupational silica exposure and chronic kidney disease. *Renal Fail* 34:40–46. doi:10.3109/0886022X.2011.623496.

Winterbourn, C. C., and D. Metodiewa. 1999. Reactivity of biologically important thiol compounds with superoxide and hydrogen peroxide. *Free Radical Biology & Medicine* 27:322–328. doi:10.1016/S0891-5849(99)00051-9.

Xu, H., F. Yang, Y. Sun, Y. Yuan, H. Cheng, Z. Wei, S. Li, T. Cheng, D. Brann, and R. Wang. 2012. A new antifibrotic target of Ac-SDKP: Inhibition of myofibroblast differentiation in rat lung with silicosis. *PLoS One* 7:e40301. doi:10.1371/journal.pone.0040301.

Yamaji-Kegan, K., Q. Su, D. J. Angelini, H. C. Champion, and R. A. Johns. 2006. Hypoxia-induced mitogenic factor has proangiogenic and proinflammatory effects in the lung via VEGF and VEGF receptor-2. *American Journal Physiological Lung Cellular Molecular Physiological* 291:L1159–L1168. doi:10.1152/ajplung.00168.2006.

Yamamoto, A., R. Takeya, M. Matsumoto, K. I. Nakayama, and H. Sumimoto. 2013. Phosphorylation of Noxo1 at threonine 341 regulates its interaction with Noxa1 and the superoxide-producing activity of Nox1. *The FEBS Journal* 280:5145–5159. doi:10.1111/febs.2013.280.issue-20.